Revisiting classical concepts of Linear Elastic Fracture Mechanics - Part II: Stretching finite strips weakened by single edge parabolically-shaped notches

Christos F. Markides
National Technical University of Athens, School of Applied Mathematical and Physical Sciences, Department of Mechanics, Zografou Campus, 5 Heroes of Polytechneion Avenue, 157 73, Attiki, Greece
markidih@maill.ntua.gr, http://orcid.org/0000-0001-6547-3616

Stavros K. Kourkoulis
National Technical University of Athens, School of Applied Mathematical and Physical Sciences, Department of Mechanics, Laboratory of Strength and Materials, Zografou Campus, 5 Heroes of Polytechneion Avenue, 157 73, Attiki, Greece
stakkour@central.ntua.gr, http://orcid.org/0000-0003-3246-9308

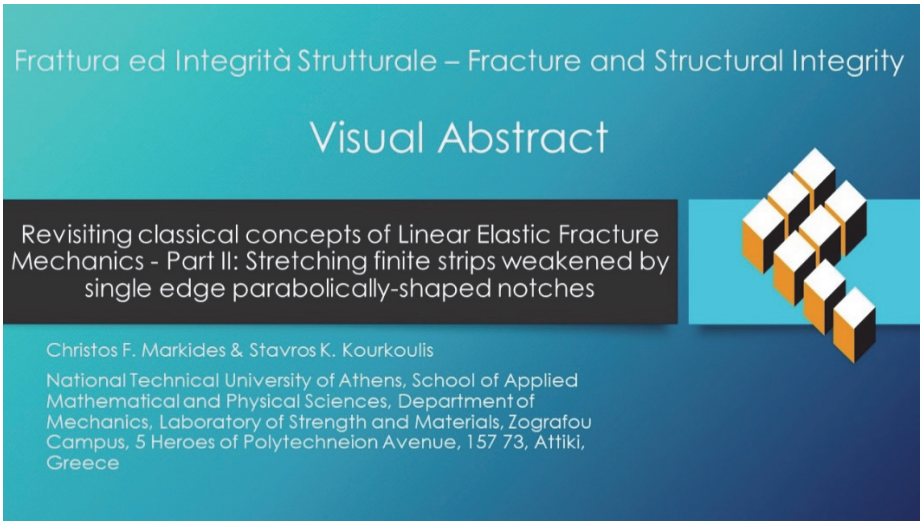

Citation: Kourkoulis, S.K., Markides, Ch.F, Revisiting classical concepts of Linear Elastic Fracture Mechanics-Part II: Mode I stress concentrations in single and double notched strips, Frattura ed Integrità Strutturale, 68 (2024) 1-18.

Received: 14.12.2023
Accepted: 05.01.2024
Published: 11.01.2024
Issue: 04.2024

KEYWORDS. Linear Elastic Fracture Mechanics, Parabolically-shaped notches, Single edge notched strip, Mode-I loading, Stress Concentration Factor, Stress Intensity Factor, Complex potentials.

INTRODUCTION

This is the second part of a short three-paper series, the aim of which is to revisit some classical concepts of Linear Elastic Fracture Mechanics (LEFM). In the first paper of the series [1] some controversial issues were discussed, related to: (i) the unnatural overlapping of the lips of 'mathematical' cracks in 'infinite plates' (a phenomenon that is predicted by the solution of the respective first fundamental problem of LEFM, in case it is formalistically applied), and, (ii) the closely associated issue of negative mode-I Stress Intensity Factors (SIFs). It could be counterargumented of course

that concepts like 'infinite plate' and 'mathematical' cracks are of limited applicability in practical engineering problems (where neither the size of actual structural members is infinite nor the discontinuities are 'mathematical' cuts with singular point tips). In spite of this skepticism, it was highlighted in ref. [1] that the solutions of LEFM, if properly adjusted, can provide interesting results, also, for actual structures. In this context, an attempt is described here to relief the suffocating assumptions of 'mathematical' discontinuities and 'infinite' media, by considering a uniaxially stretched plane strip of finite dimensions weakened by a notch of parabolic shape.

The distinction between cracks and notches (either sharp or blunt) concerns the engineering community long ago. In fact, it can be stated that the magnificent history of Fractures Mechanics started with the pioneering study of Inglis, related to the stress concentration at the apex of elliptical holes [2]. The importance of flaws in the form of 'mathematical' cracks (rather than of notches) was highlighted a few years later [3], when Griffith performed his well-known experiments with specimens made of glass [4]. Based on the data gathered, he concluded that the "... *weakness* (of the specimens tested) *is due almost entirely to minute cracks in the surface* ..." [5]. From this instant on, the main challenge was the description of the stress fields that are developed in the immediate vicinity of the tips of 'mathematical' cracks or sharp notches (V-shaped notches) and around the 'crowns' of blunted notches (either U- or hyperbolically-shaped). The main difference between the two cases is that around the tip of sharp discontinuities the stress field components attain infinite values while around the crown of blunt notches the stresses remain bounded.

Although it may be considered a paradox, the problem of the stress field around sharp discontinuities was proven to be easier (at least under the assumption of linear elasticity), and its solution was essentially facilitated by the concept of the Stress Intensity Factor, introduced by Irwin [6]. Using the SIF concept and taking advantage of Westergaard's work [7], Irwin provided, already at the late fifties, compact and relatively flexible equations for the stress components around the tips of 'mathematical' cracks as the first terms of a series expansion. Around the same period, Williams [8, 9] published his seminal papers with the familiar equations for the stress field around sharp V-notches, in terms of eigenfunction series expansions. Almost simultaneously, Neuber [10] dealt with the stress concentration factors for notched bodies, of various geometries under various loading schemes, adopting Airy's biharmonic potential functions. For the next decades Neuber's books became reference points for engineers dealing with problems of practical interest. Equations similar to the ones introduced by Williams [8, 9] were presented almost thirty years later by Carpenter [11], who adopted the technique of complex potentials, developed by Kolosov [12] and Muskhelishvili [13].

On the other hand, the respective problem for blunt discontinuities was proven rather tougher. Even today, contributions providing reliable, full-filed, closed form solutions of the problem are mostly welcome. Creager and Paris are, perhaps, the first ones to tackle the problem, in their effort to confront stress corrosion cracking, i.e. "...*growth of cracks due to the combined and interrelated action of stress and environment* ..." [14]. According to their approach, corrosion cracking is responsible for the generation of discontinuities in the form of "... *an elliptical or hyperbolic cylinder ... in which the radius of curvature at the tip is small in comparison to the major dimensions of the void* ..." and not in the form of the "... *usual plane ending with zero radius of curvature* ..." [14]. They concluded that the respective stress field in the immediate vicinity of the crown of the blunt notch can be still described by means of a 'generalized' SIF, assuming that the Cartesian reference system is translated from the tip of the ellipse to its focal point. Some twenty years later, simplified expressions for the respective stress field components were obtained by Glinka [15], in terms of the stress concentration factor, the radius of the crown of the notch and the distance from it (keeping the exponents of the distance from the tip of the notch unaltered). Although it was reported that these simplified formulae provided results in good agreement with the respective ones obtained numerically by means of the Finite Element technique, Lazzarin and Tovo [16] indicated that Glinka's statement about the 'universality' of the notch stress fields are incompatible to Williams' [8, 9] conclusions concerning the dependence of the singularity degree on the opening angle of the notch. In other words, Lazzarin and Tovo [16] suggested that Glinka's formulae are valid exclusively for notches with zero opening angles. Some years later, the problem was tackled, also, by Nui et al. [17], who presented a solution for the stress field in a finite plane weakened by a single edge V-shaped notch with rounded tip. The solution was achieved using a modified Schwartz-Cristoffel transformation in parallel with Muskhelishvili's technique [13].

The last decade of the 20th century is signaled by the contributions of Lazzarin's scientific team, which, are, perhaps, the most influential ones on the issue of the stress fields around either blunt or sharp notches. They dealt not only with the description of the stress components but they contributed, also, in the direction of understanding the conditions causing fracture of notched structural members either under static or fatigue loading schemes. Having as starting point the study of welded lap joints under fatigue conditions [18], they presented flexible approximate solutions for the components of the stress field in the vicinity of open notches, adopting the complex potential's technique [16]. Later, their approximate solutions [16] were improved, taking into account, also, rounded V-shaped notches with large opening angles [19]. In general, they considered a broad variety of geometrical configurations [20] (including even finite domains [21]), discussing their potential influence on the fatigue limit predictions. In addition, they contributed significantly to the development of

the 'generalized stress intensity factor' concept, both for rounded V-shaped notches [22] and, also, for U-shaped ones [23]. Later on, their attention was focused on the fracture of notched members, both experimentally and analytically, by means of proper fracture criteria, either energy- or stress-based [24-28].

Concluding this short review, it becomes evident that the interest on the issue of the stress field around various types of notches is continuous and uninterrupted since it was discussed for the first time, due to its paramount importance for the solution of practical engineering problems. The topic is even today under intensive study. In most cases the stress field used is that introduced by the scientific team of late Professor Lazzarin [19, 22]. Indicatively only, one could mention the contributions by Chen and Fan [29], who attempted estimation of fracture loads for blunt U-shaped notches by means of two fracture criteria, adopting the equations for the stress field provided by Lazzarin and Filippi [22]. Recently, Ghadirian et al. [30] determined the mode-I fracture toughness of rock like materials using the notched Brazilian disc configuration and the stress field introduced by Filippi et al. [19]. The same field was used by Sangsefidi et al. [31], who determined the mixed-mode fracture toughness of rocks, again by means of the Brazilian disc test with specimens weakened by U-shaped notches. Nowadays, hybrid schemes are extensively used, combining successfully analytical solutions with experimental protocols and numerical tools [32-34].

In the light of the above discussion, it can be definitely stated that the question concerning the stress field in the vicinity of the crown of notched members is by no means closed. In this context, an alternative approach is presented in this study for the analytical confrontation of the problem, based on a proper conformal mapping and the complex potentials technique [13]. The novelty of the present approach is its capability to deal with finite domains and parabolically shaped notches, independently of the specimen-notch relative dimensions. Moreover, the formulae provided for the components of the stresses are full-field and of closed form. Results of the present solution were comparatively considered against the ones obtained by the respective solution by Filippi et al. [19], for similar geometrical configurations and loading schemes. The agreement is proven quite satisfactory, at least from the qualitative point of view. The same is true for the comparison of the results of the present solution against those of a numerical project that is in progress [35].

THEORETICAL CONSIDERATIONS

The problem

The first fundamental problem of plane elasticity of a finite strip (length: 2b, width: 2h), weakened by a stress-free edge notch, of parabolic shape L, is analytically explored in this study. The strip is uniaxially stretched by means of a uniform stress distribution $\sigma_{xx}=\sigma_o$ ($\sigma_o>0$) that is applied all along its width 2h, as it is shown in Fig.1. The axis of symmetry of the parabola is, also, axis of symmetry of the strip and it coincides with the y-axis of the Cartesian reference system xOy, while the load is applied along the x-axis of the system.

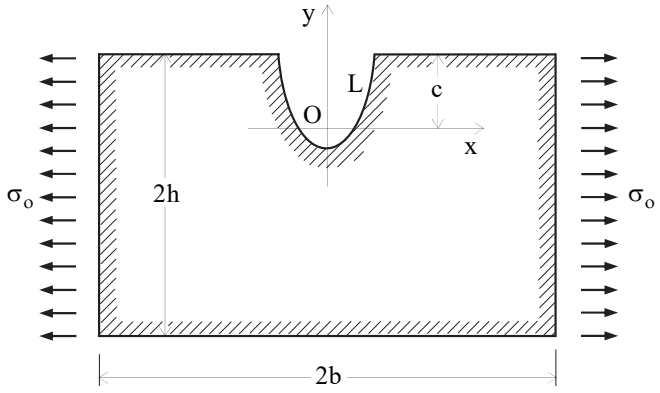

Figure 1: The configuration of the problem.

Assuming further that the material of the strip is linearly elastic, isotropic and homogeneous, Muskhelishvili's complex potentials technique is adopted. In this context, use is made of the following analytic function $\omega(\zeta)$ [13]:

$$z=\omega(\zeta)=i(\zeta-i\alpha)^2;\quad z=x+iy=i(\xi+i\eta-i\alpha)^2;\quad x=2(\alpha-\eta)\xi;\quad y=\xi^2-(\alpha-\eta)^2 \tag{1}$$

This function maps conformally the region of the plane $z=x+iy=re^{i\theta}$ that lies outside of the parabola L with equation:

$$x = 2\alpha\sqrt{\alpha^2 + y} \tag{2}$$

to the mathematical lower half plane of the complex variable $\zeta=\xi+i\eta$. In other words, orthogonal parabolas in the z plane (with their focus at the origin O of the (x, y) Cartesian reference system), defining a curvilinear reference system (ξ, η) in the z plane (Fig.2a), correspond to orthogonal lines in the mathematical lower half plane (Fig.2b). In this way, the vertex (or base-point or tip), $z(0, -\alpha^2)$ of the parabola L, corresponds to the point $\zeta(0, 0)$ in the mathematical plane. A finite part, of dimensions 2bx2h, of the z plane (bounded by red lines in Fig.2a), containing a finite part of the parabola L, represents the region of the edge notched strip under study.

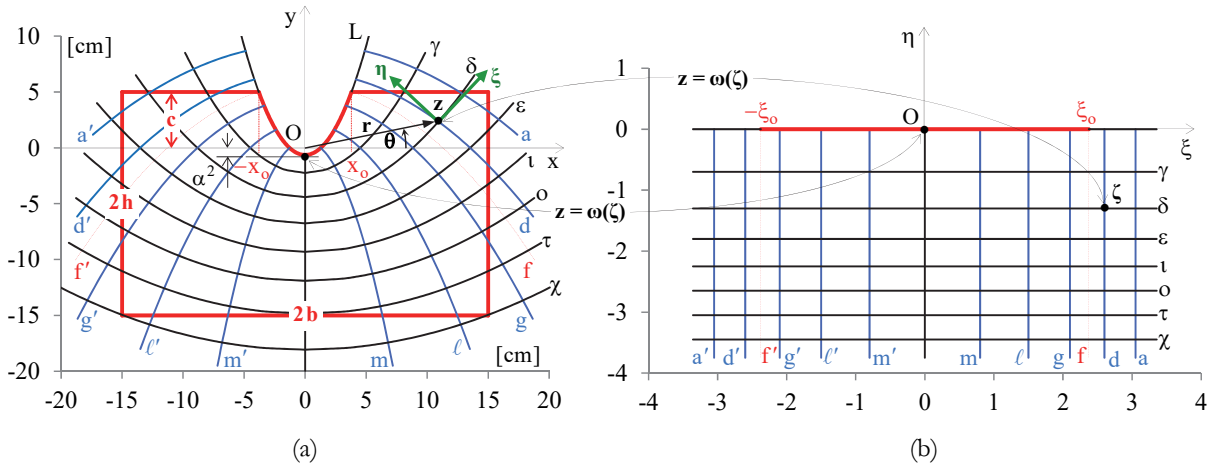

Figure 2: The conformal mapping of the actual plane z with the notched strip (a) on to the mathematical lower half plane ζ (b).

For the sake of generality, the x-axis is not considered as symmetry axis of the strip, but rather it is located at a distance c from its upper side. In this context, the two end points of the parabolically shaped notch are $(-x_o, c)$, (x_o, c) (Fig.2a), while the notch itself is reflected to the linear segment (marked red in Fig.2b) defined by the two end points $(-\xi_o, 0)$, $(\xi_o, 0)$ in the mathematical plane $\zeta=\xi+i\eta$.

Outline of the method

To obtain the solution for the stress field developed in the notched stretched strip, an intact strip of the same dimensions 2bx2h stretched by the uniformly distributed tensile stresses $\sigma_o>0$, is considered first. Obviously, at any point of this intact strip (and, therefore, at any point of an internal parabolic locus L), the stress field is described by a uniaxial tensile stress, $\sigma_{xx}=\sigma_o>0$, while it holds that $\sigma_{yy}=\sigma_{xy}=0$ (Fig.3a). The solution of this auxiliary problem in terms of the variable ζ in the mathematical plane will be determined in terms of the functions $\Phi_1(\zeta)$, $\Psi_1(\zeta)$.

As a next step, consider the opposite stress field, applied at all the points of the internal locus L, i.e., $\sigma_{xx}= -\sigma_o$, analyzed into components $\sigma_{\eta\eta}$, $\sigma_{\xi\eta}$ in the (ξ, η) curvilinear system, mentioned previously (Fig.3b). Let us now set these $\sigma_{\eta\eta}$, $\sigma_{\xi\eta}$ as the boundary stresses on the parabolic notch L of a notched strip 2bx2h with stress free sides (Fig.3c), and denote by $\Phi_2(\zeta)$, $\Psi_2(\zeta)$ the functions solving the specific problem. Then, the solution for the edge notched strip into question, i.e., the finite strip subjected to uniform tension σ_o on its sides and weakened by a stress free parabolically-shaped notch L, is obtained by simply superposing the previous two solutions ($\Phi_1(\zeta)$, $\Psi_1(\zeta)$) and ($\Phi_2(\zeta)$, $\Psi_2(\zeta)$), as it is shown schematically in Fig.3d).

$$\Phi(\zeta) = \Phi_1(\zeta) + \Phi_2(\zeta), \quad \Psi(\zeta) = \Psi_1(\zeta) + \Psi_2(\zeta) \tag{3}$$

The above procedure and the particular solutions $\Phi_1(\zeta)$, $\Psi_1(\zeta)$ and $\Phi_2(\zeta)$, $\Psi_2(\zeta)$, are explicitly described in next sections.

In order for the above described method to be better understood it is deemed necessary, to highlight some crucial points of the superposition procedure proposed. The underlying idea is to somehow reach the configuration and solution of a parabolically notched strip by 'introducing' the notch to the respective intact stretched strip (Fig.3a). This is here achieved by imposing an opposite stress field $-\sigma_o$ at the points of the internal locus L of the intact stretched strip. In fact, such an imposition of $-\sigma_o$ on the locus L of the intact stretched strip (Fig.3b), cancels the tensile stress σ_o along L, rendering the

area enclosed by L and the upper boundary of the strip stress free (or, equivalently, this area is 'neutralized'). Actually, this can be conceived as if the specific area had been removed from the strip, thus, transforming it into the notched one.

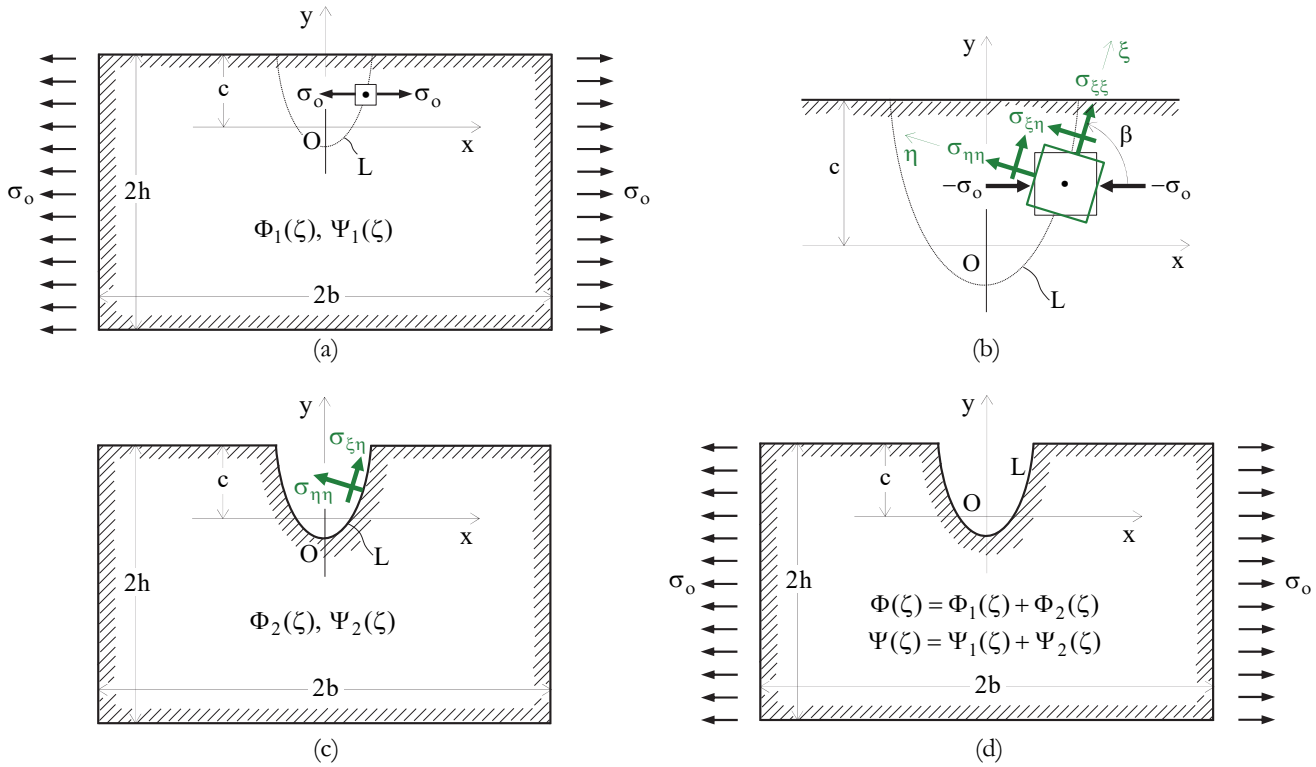

Figure 3: (a) The problem of the stretched intact strip under direct uniaxial tension and the stress field along the internal parabolic locus L; (b) The opposite stress field applied at all the points of the internal locus L; (c) The problem of the notched strip under the opposite stress field on the boundary of the notch L and stress free sides; (d) The stretched, parabolically notched strip obtained by the superposition of the problems (a) and (c).

The question arising now is how could this 'neutralization' be implemented? A direct approach is by using the principle of superposition, holding for a linearly elastic behavior of the strip, i.e., by superposing to the initial problem of stretching of the intact strip a problem that induces a $-\sigma_o$ stress along L. But the $-\sigma_o$ stress field acting along the internal locus L could only be achieved by considering the problem of the intact strip acted by $\sigma_{xx}=-\sigma_o$ on its loaded sides, which upon being superimposed to the stretched strip (by $\sigma_{xx}=\sigma_o$) would lead to the unstressed strip (i.e., there would be no problem). For this reason, it was necessary to consider the notched strip with stress free sides, loaded along its notch L by the boundary stresses $\sigma_{\eta\eta}$, $\sigma_{\xi\eta}$ (Fig.3c), which correspond to the $-\sigma_o$ stress field (Fig.3b). Then, the superposition of the problems shown in Figs.3a and 3c, suffices for both the zeroing of stresses along L in the intact strip (indirectly transforming it into the notched one), and, also, for the achievement of the required loading scheme (i.e., that of a tensile uniform stress σ_o at the loaded boundaries of the strip).

Obviously, the above-described procedure is essentially a superposition of complex potentials, $\Phi_1(z)+\Phi_2(z)$, $\Psi_1(z)+\Psi_2(z)$, namely, the perturbation to the stress field due to $\Phi_1(z)$, $\Psi_1(z)$ that is caused by $\Phi_2(z)$, $\Psi_2(z)$, which are responsible for the stress vanishing along L. Furthermore, this procedure is well conceived as an extension of the respective one introduced in Muskhelishvili's [13] milestone book. Indeed, according to Muskhelishvili, the configuration of a perforated infinite strip is achieved by considering the intact strip, an internal boundary L in the location of the perforation, and, then by mapping conformally the area outside of L onto the infinite plane with the unit hole, and, finally, by demanding L to be free from stresses (thus, rendering the intact infinite strip a perforated one). The above assumptions and the respective analytical solutions introduced in next sections are validated by comparing their outcomes against those provided by well-established solutions, for similar geometries and loading schemes, as well as against a numerical solution in progress.

Stretching of the intact strip

It is easily seen that the complex potentials solving the problem of stretching an intact strip 2bx2h by a stress σ_o, which is uniformly applied along its vertical edges (Fig.3a), read as:

$$\Phi_1(z)=\Phi_1(\omega(\zeta))=\Phi_1(\zeta)=\frac{\sigma_o}{4},\quad \Psi_1(z)=\Psi_1(\omega(\zeta))=\Psi_1(\zeta)=-\frac{\sigma_o}{2} \tag{4}$$

Indeed, substituting Eqns.(4) into the familiar formulae providing stresses in terms of $\Phi_1(z)$, $\Psi_1(z)$ in the actual domain, i.e.:

$$\sigma_{xx}+\sigma_{yy}=4\Re\Phi_1(z),\quad \sigma_{yy}-i\sigma_{xy}=2\Re\Phi_1(z)+z\overline{\Phi_1'(z)}+\overline{\Psi_1(z)} \tag{5}$$

(where $\Re$ denotes the real part; prime denotes the first order derivative and over-bar denotes the conjugate complex value [13]), it follows that at every point of the intact strip it holds that $\sigma_{xx}=\sigma_o>0$, $\sigma_{yy}=\sigma_{xy}=0$, as it was expected, and, obviously, the same stresses appear all along the internal parabola L of the strip (Fig.3a).
Consider now the opposite stress field, i.e.:

$$\sigma_{xx}=-\sigma_o,\quad \sigma_{yy}=\sigma_{xy}=0 \tag{6}$$

Substituting from Eqns.(6) in the transformation formulae [13]:

$$\sigma_{\eta\eta}+\sigma_{\xi\xi}=\sigma_{yy}+\sigma_{xx},\quad \sigma_{\eta\eta}-\sigma_{\xi\xi}+2i\sigma_{\xi\eta}=(\sigma_{yy}-\sigma_{xx}+2i\sigma_{xy})e^{2i\beta} \tag{7}$$

one obtains the respective stress components in the (η, ξ) curvilinear system, rotated by an angle β with respect to the x-axis (Fig3.b), as:

$$\sigma_{\eta\eta}+\sigma_{\xi\xi}=-\sigma_o \tag{8}$$

$$\sigma_{\eta\eta}-\sigma_{\xi\xi}+2i\sigma_{\xi\eta}=\sigma_o e^{2i\beta} \tag{9}$$

Taking into account that [13]:

$$e^{2i\beta}=\frac{\omega'(\zeta)}{\overline{\omega'(\zeta)}}\overset{\text{Eqns.(1)}}{=}-\frac{\zeta-i\alpha}{\overline{\zeta}+i\alpha} \tag{10}$$

Eqn.(9) becomes:

$$\sigma_{\eta\eta}-\sigma_{\xi\xi}+2i\sigma_{\xi\eta}=-\sigma_o\frac{\zeta-i\alpha}{\overline{\zeta}+i\alpha} \tag{11}$$

Adding Eqns.(8) and (11), and recalling that $\zeta=\xi+i\eta$, yield:

$$\sigma_{\eta\eta}+i\sigma_{\xi\eta}=-\sigma_o\frac{\xi^2+i\xi(\eta-\alpha)}{\xi^2+(\eta-\alpha)^2} \tag{12}$$

In particular, for $\eta=0$, Eqn.(12) provides (after separating the real from the imaginary part) the $\sigma_{\eta\eta,L}$ and $\sigma_{\xi\eta,L}$ components of the stress field at the points of the internal parabola L, due to the opposite stress field of Eqns.(6), as:

$$\sigma_{\eta\eta,L}=-\sigma_o\frac{\xi^2}{\xi^2+\alpha^2},\quad \sigma_{\xi\eta,L}=\sigma_o\frac{\alpha\xi}{\xi^2+\alpha^2} \tag{13}$$

The notched strip with stress free sides loaded by certain stresses along the parabolic notch L
Consider now the first fundamental problem of a strip 2bx2h with stress free linear edges, baring a parabolically shaped edge notch L acted by the previous stresses $\sigma_{\eta\eta,L}$ and $\sigma_{\xi\eta,L}$ of Eqns.(13) (Fig.3c). The solution of this problem, in terms of

the variable $\zeta=\xi+i\eta$ (via the mapping of Eqns.(1)), is expressed in terms of $\Phi_2(\zeta)$, $\Psi_2(\zeta)$. Taking into account Eqns.(1) for $\eta=0$, and Eqns.(13), the boundary condition for the stresses on the parabolic notch L reads, in terms of the two functions Φ_2 and Ψ_2, as follows:

$$(\xi+i\alpha)\Phi_2(\xi)+(\xi+i\alpha)\overline{\Phi_2(\xi)}+\frac{(\xi+i\alpha)^2}{2}\Phi_2'(\xi)-(\xi-i\alpha)\Psi_2(\xi)=-\sigma_o\xi \tag{14}$$

Following Muskhelishvili [13], the solution to the functional equation of Eqn.(14) is:

$$\Phi_2(\zeta)=\frac{1}{2\pi i(\zeta-i\alpha)}\int_{-\xi_o}^{\xi_o}\frac{\sigma_o\xi d\xi}{\xi-\zeta},\quad \Psi_2(\zeta)=\frac{-1}{2\pi i(\zeta-i\alpha)}\int_{-\xi_o}^{\xi_o}\frac{\sigma_o\xi d\xi}{\xi-\zeta}+\frac{\zeta+i\alpha}{\zeta-i\alpha}\Phi_2(\zeta)+\frac{(\zeta+i\alpha)^2}{2(\zeta-i\alpha)}\Phi_2'(\zeta) \tag{15}$$

After some relatively lengthy algebra it is obtained that:

$$\Phi_2(\zeta)=\frac{\sigma_o}{2\pi i(\zeta-i\alpha)}\left(\zeta\log\frac{\zeta-\xi_o}{\zeta+\xi_o}+2\xi_o\right) \tag{16}$$

$$\Psi_2(\zeta)=\frac{\sigma_o}{2\pi i}\left[\frac{3i\alpha\zeta^2+6\alpha^2\zeta+i\alpha^3}{2(\zeta-i\alpha)^3}\log\frac{\zeta-\xi_o}{\zeta+\xi_o}-\frac{\zeta^2-2i\alpha\zeta-5\alpha^2}{(\zeta-i\alpha)^3}\xi_o+\frac{\zeta(\zeta+i\alpha)^2}{2(\zeta-i\alpha)^2}\left(\frac{1}{\zeta-\xi_o}-\frac{1}{\zeta+\xi_o}\right)\right] \tag{17}$$

Stretching of the strip with the stress free edge notch L

Substituting from Eqns.(4), (16) and (17) in Eqn.(3), the solution of the problem in question (i.e., that of stretching a finite strip 2bx2h with the stress free edge notch L, (Fig.3d or Fig.1)), is obtained as:

$$\Phi(\zeta)=\frac{\sigma_o}{4}+\frac{\sigma_o}{2\pi i(\zeta-i\alpha)}\left(\zeta\log\frac{\zeta-\xi_o}{\zeta+\xi_o}+2\xi_o\right) \tag{18}$$

$$\Psi(\zeta)=-\frac{\sigma_o}{2}+\frac{\sigma_o}{2\pi i}\left[\frac{3i\alpha\zeta^2+6\alpha^2\zeta+i\alpha^3}{2(\zeta-i\alpha)^3}\log\frac{\zeta-\xi_o}{\zeta+\xi_o}-\frac{\zeta^2-2i\alpha\zeta-5\alpha^2}{(\zeta-i\alpha)^3}\xi_o+\frac{\zeta(\zeta+i\alpha)^2}{2(\zeta-i\alpha)^2}\left(\frac{1}{\zeta-\xi_o}-\frac{1}{\zeta+\xi_o}\right)\right] \tag{19}$$

Inversing the transformation of Eqns.(1) yields:

$$\zeta=i\alpha+\sqrt{-iz} \tag{20}$$

Substituting for ζ from Eqn.(20) in Eqns.(18) and (19), the solution in terms of the variable $z=x+iy=re^{i\theta}$ is obtained as:

$$\Phi(z)=\frac{\sigma_o}{4}+\frac{\sigma_o}{2\pi i}\sqrt{\frac{i}{z}}\left[\left(i\alpha+\sqrt{-iz}\right)\log\frac{i\alpha+\sqrt{-iz}-\xi_o}{i\alpha+\sqrt{-iz}+\xi_o}+2\xi_o\right] \tag{21}$$

$$\begin{aligned}\Psi(z)=-\frac{\sigma_o}{2}+\frac{\sigma_o}{4\pi}\Bigg\{&\frac{3\alpha z+4i\alpha^3}{z^{3/2}}\sqrt{i}\log\frac{i\alpha+\sqrt{-iz}-\xi_o}{i\alpha+\sqrt{-iz}+\xi_o}+\frac{iz+4\alpha^2}{z^{3/2}}2\sqrt{i}\,\xi_o\\&+\frac{5\alpha z-iz\sqrt{-iz}-8\alpha^2\sqrt{-iz}-4i\alpha^3}{\left(i\alpha+\sqrt{-iz}\right)^2-\xi_o^2}\frac{2\xi_o}{z}\Bigg\}\end{aligned} \tag{22}$$

The stress field in the stretched notched strip

At one's convenience, the stress components in the stretched, notched strip (Fig.1 or Fig.3d), may be expressed either in the Cartesian (x, y) or the curvilinear (ξ, η) reference sytem, via the well-known formulae [13]:

$$\sigma_{yy} - i\sigma_{xy} = 2\Re\Phi(z) + z\overline{\Phi'(z)} + \overline{\Psi(z)}, \quad \sigma_{xx} = 4\Re\Phi(z) - \sigma_{yy} \tag{23}$$

$$\sigma_{\eta\eta} - i\sigma_{\xi\eta} = 2\Re\Phi(\zeta) + \frac{\overline{\omega(\zeta)}}{\overline{\omega'(\zeta)}}\Phi'(\zeta) + \frac{\omega'(\zeta)}{\overline{\omega'(\zeta)}}\Psi(\zeta), \quad \sigma_{\xi\xi} = 4\Re\Phi(\zeta) - \sigma_{\eta\eta} \tag{24}$$

In this context, substituting from Eqns.(21, 22) in Eqns.(23), the explicit expressions for the Cartesian stress components σ_{xx}, σ_{yy}, σ_{xy}, in terms of $z=x+iy=re^{i\theta}$, at any point (r, θ) in the notched strip, are obtained. The respective (rather lengthy) full-field and closed-form expressions are given in Appendix. In particular, regarding the stress field along the notch L, the curvilinear system (ξ, η) appears to be more convenient than the Cartesian one. In this context, substituting from Eqns.(18, 19) into Eqns.(24), setting $\zeta=\xi$ (i.e., $\eta=0$), and taking into account that by the fourth of Eqns.(1) it holds that $\xi=(\alpha^2+y)^{1/2}$ and $\xi_o=(\alpha^2+c)^{1/2}$, it follows that:

$$\sigma_{\xi\xi} = \sigma_o + \frac{2\sigma_o}{\pi\left(2\alpha^2+y\right)}\left[\alpha\left(\sqrt{\alpha^2+y}\log\frac{\sqrt{\alpha^2+c}-\sqrt{\alpha^2+y}}{\sqrt{\alpha^2+c}+\sqrt{\alpha^2+y}} + 2\sqrt{\alpha^2+c}\right) - \pi\left(\alpha^2+y\right)\right], \quad -\alpha^2 \le y < c \tag{25}$$

$$\sigma_{\xi\eta} = \sigma_{\eta\eta} = 0 \tag{26}$$

Eqns.(26) were expected, expressing the fulfillment of the notch stress free boundary conditions. Regarding $\sigma_{\xi\xi}$, as it is seen from Eqn.(25), becomes singular for y=c, i.e., at the end points of the notch L (i.e., at the points of intersection of L with the upper edge of the strip). However, as it will be proven in next sections, $\sigma_{\xi\xi}$ remains bounded even infinitesimally close to the notch end points, e.g. considering a value $y \le 0.99c$, the one that will be adopted in the next applications.

EXPLORING THE STRESS FIELD ALONG SOME STRATEGIC LOCI – VALIDATION OF THE SOLUTION

In the following examples, the variation of the stress field components is plotted along some strategic loci, i.e., along the boundaries of the strip, along the bisector of the notch and, also, along the flanks of the notch, in an attempt to highlight the potentials of the solution and, also, to explore critical features of the respective distributions, regarding the fulfillment of the boundary conditions imposed. Moreover, the variation of the polar stress components is plotted in the immediate vicinity of the notch base (or notch tip), in order for the present solution to be compared against the well-established one provided analytically and numerically by Filippi et al. [19].

Due to symmetry, all plots are realized only for the half strip. Along the strip sides and the notch bisector (i.e., y-axis), use was made of the expressions of the Appendix. As already mentioned, in order to avoid the singularity at the end points of the notch $(\pm x_o, c)$, y was set equal to 0.99c, instead of c, all along the upper side of the strip. For the plots along the half notch, use was made of Eqn.(25) for the only non-zero stress component $\sigma_{\xi\xi}$. A strip of dimensions 2bx2h=(30x20) cm was considered. The x-axis was constantly located at a fixed distance c=5 cm from the upper strip side. Three characteristic geometries were considered for the notch, depending on the value of α of Eqn.(2); namely, for α=0.25, 0.5 and 1.0 $cm^{1/2}$, corresponding to notches becoming gradually deeper (longer) and wider (as it can be seen in the figures of the following sections). In all cases, the strip was stretched by a uniformly distributed tensile stress $\sigma_{xx}=\sigma_o$=10 MPa, applied along its vertical edges (normally to the direction of the bisector of the notch).

Stresses along the strip edges, the notch bisector and the notch flanks

In Fig.4, the variation of the σ_{xx} stress (red color) along the sides of the strip and along the bisector of the notch is plotted, together with the variation of the $\sigma_{\xi\xi}$ stress component (green color) along the flank of the notch, for three characteristic α-values. The stresses are properly adjusted to the length scale considered in the plots, providing a better overview of their variations along the 2bx2h strip. Some characteristic numerical values for the stresses are, also, shown in the diagrams. It is seen that even in the case of a strip of dimensions comparable to those of the notch, the applicability of the present solution is well justified. Clearly, for a bigger strip the solution will perfectly fulfill the boundary conditions imposed. It is worth mentioning, also, that the sign change of the $\sigma_{\xi\xi}$ stress component along the notch flanks, resembles the respective one observed for the distribution along the elliptic or circular holes in the case of the infinite, uniaxially stretched plate.

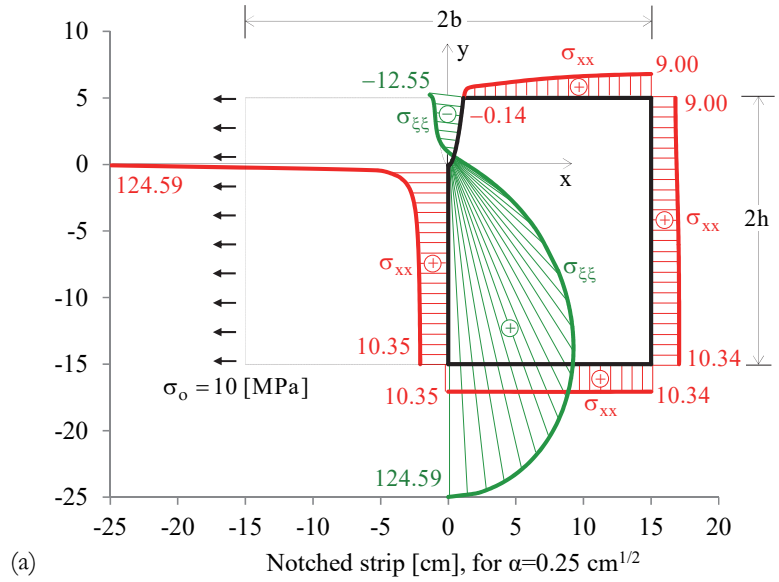

(a) Notched strip [cm], for α=0.25 cm$^{1/2}$

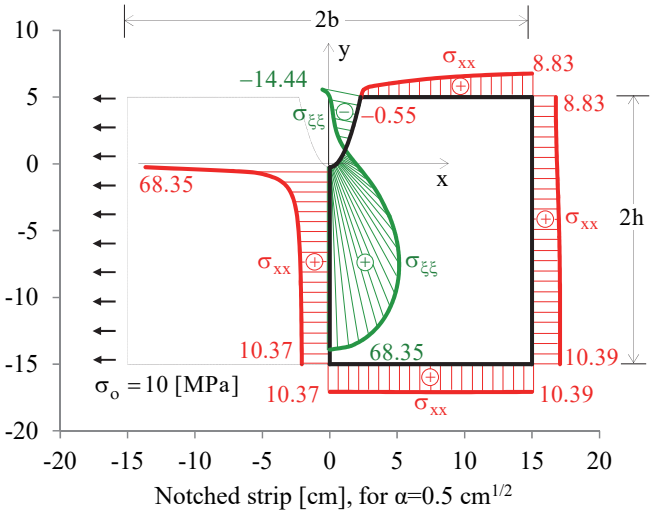

(b) Notched strip [cm], for α=0.5 cm$^{1/2}$

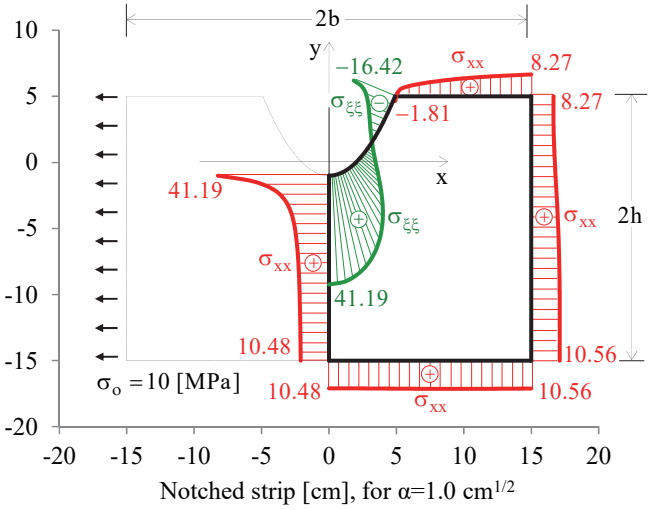

(c) Notched strip [cm], for α=1.0 cm$^{1/2}$

Figure 4: The variation of σ_{xx} along the bisector of the notch (y-axis), along the edges sides of the strip, and the variation of $\sigma_{\xi\xi}$ along half of the perimeter of the notch, for a notch with (a) α=0.25, (b) α=0.5 and (c) α=1.0 cm$^{1/2}$.

The variation of the remaining two Cartesian stress components, σ_{yy} and σ_{xy}, along the same as previously loci are shown in Fig.5. It is seen that the distributions along the strip edges fulfill (according to a quite satisfactory manner) the boundary conditions imposed. The non-zero values of σ_{yy} and σ_{xy} along the notch flanks (in the interior) are to suffice the zeroing of the boundary stress components $\sigma_{\eta\eta}$ and $\sigma_{\xi\eta}$ along the notch flank (approaching the strip from its exterior).

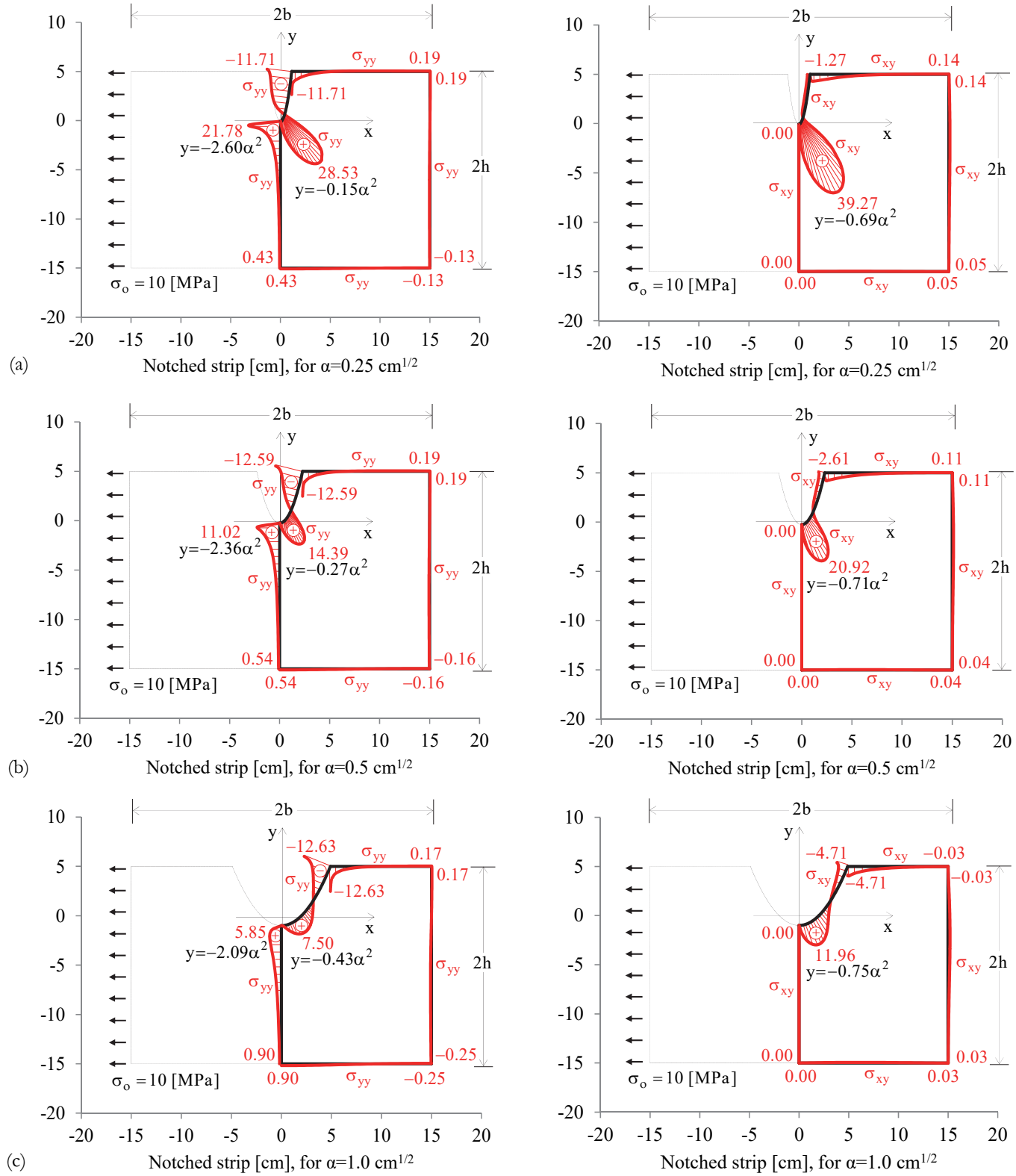

Figure 5: The variation of σ_{yy} and σ_{xy} along the bisector of the notch (y-axis), along the linear edges of the strip and along half of the perimeter of the notch, for a notch with (a) α=0.25, (b) α=0.5 and (c) α=1.0 cm$^{1/2}$.

The variation of the polar stress in the vicinity of the base (tip) of the notch

In Fig.6, the variation of the polar stress components σ_{rr}, $\sigma_{\theta\theta}$, $\sigma_{r\theta}$, is plotted along a semi-circular locus (red color) with its center at the origin of the reference system, enclosing a part of the strip in the vicinity of the base (tip) of the notch. Three different stretched, notched strip configurations are studied in accordance with the parameters set in previous section. The radii r of the circular loci around each one of the three notch bases were arbitrarily chosen as: $r=10\alpha^2$ for $\alpha=0.25$ cm$^{1/2}$, resulting to an angle range $53.13^o\leq\theta\leq-90^o$ (Fig.6a), $r=4\alpha^2$ for $\alpha=0.5$ cm$^{1/2}$ (resulting to $30^o\leq\theta\leq-90^o$) (Fig. 6b), and $r=3\alpha^2$ for $\alpha=1.0$ cm$^{1/2}$ (resulting to $19.47^o\leq\theta\leq-90^o$) (Fig.6c). For the calculations of stresses, the general expressions given in the Appendix were used, in conjunction with the transformation formulae for the rotation of the reference system at an angle θ. The distributions of σ_{rr}, $\sigma_{\theta\theta}$, $\sigma_{r\theta}$, resemble qualitatively the respective well established ones given in ref.[19], based on completely different analytical and numerical approaches, thus, justifying further the validity of the present solution.

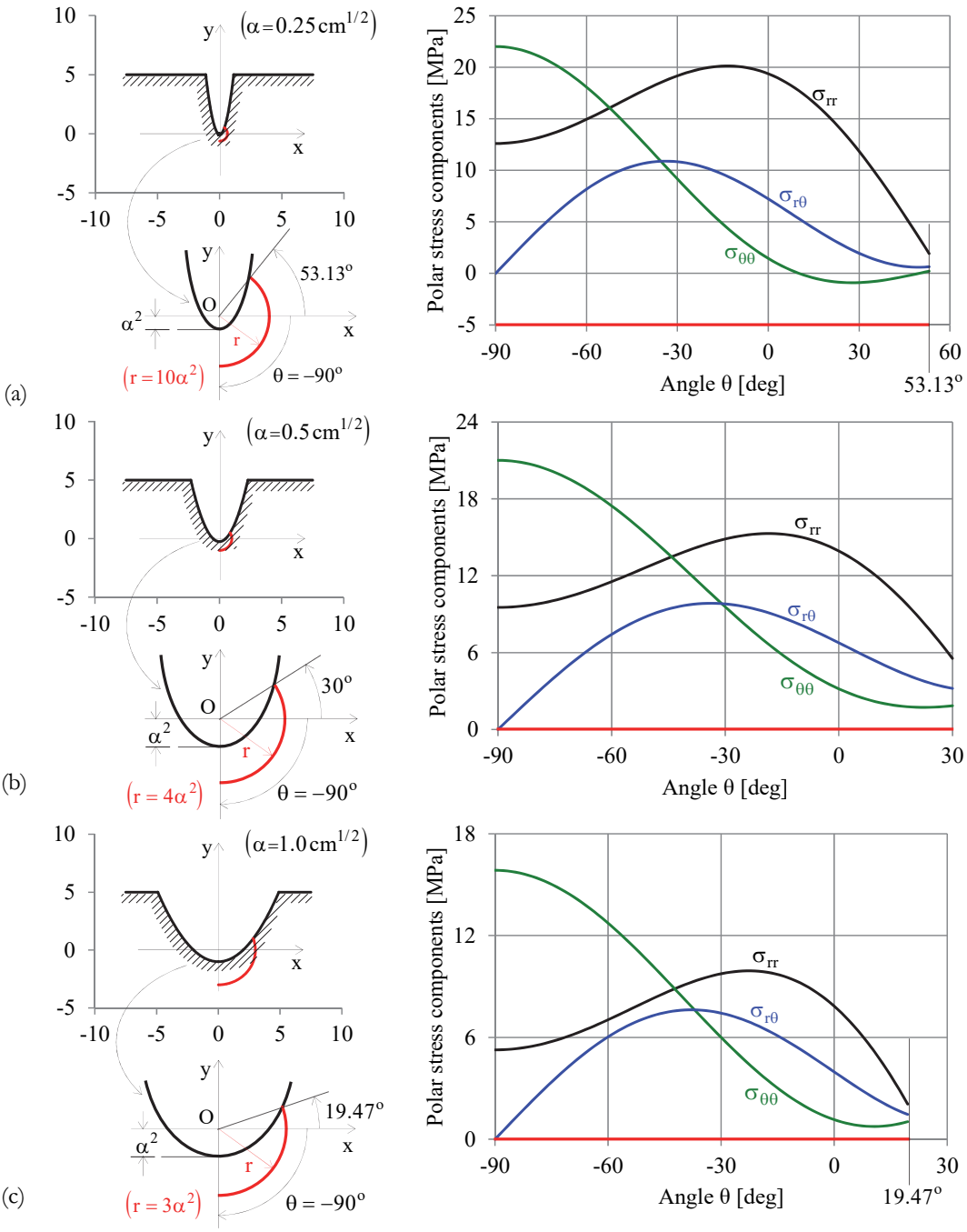

Figure 6: The variation of the σ_{rr}, $\sigma_{\theta\theta}$ and $\sigma_{r\theta}$, stress components along a circular locus around the base (tip) of the notch, for notches with (a) $\alpha=0.25$, (b) $\alpha=0.5$ and (c) $\alpha=1.0$ cm$^{1/2}$.

Stress variation along the notch bisector (y-axis)

In the present case, where the strip is stretched normally to the notch bisector, the stress field along the y-axis (aligned along the bisector of the notch) is of particular interest, since it provides among others the Stress Concentration Factor. In this direction, the reduced formulae for the Cartesian stress components are next provided along the y-axis. By setting $\theta=-\pi/2$ in the full-field expressions of the Appendix, it is obtained that:

$$\sigma_{xx}=\sigma_o+\frac{2\sigma_o}{\pi}\left[\frac{\alpha}{\sqrt{r}}\left(\frac{\sqrt{r}}{\alpha}-\frac{\alpha^2}{r}\right)\left(\tan^{-1}\frac{\sqrt{r}-\alpha}{\xi_o}-\frac{\pi}{2}\right)+\left(1+\frac{\alpha^2}{r}\right)\frac{\xi_o}{\sqrt{r}}+\alpha\left(1-\frac{\alpha}{\sqrt{r}}\right)^2\frac{\xi_o}{\xi_o^2+\left(\sqrt{r}-\alpha\right)^2}\right] \tag{27}$$

$$\sigma_{yy}=\frac{2\sigma_o}{\pi}\left[\frac{\alpha}{\sqrt{r}}\left(\frac{\sqrt{r}}{\alpha}+\frac{\alpha^2}{r}-2\right)\left(\tan^{-1}\frac{\sqrt{r}-\alpha}{\xi_o}-\frac{\pi}{2}\right)+\left(1-\frac{\alpha^2}{r}\right)\frac{\xi_o}{\sqrt{r}}-\alpha\left(1-\frac{\alpha}{\sqrt{r}}\right)^2\frac{\xi_o}{\xi_o^2+\left(\sqrt{r}-\alpha\right)^2}\right] \tag{28}$$

$$\sigma_{xy}=0 \tag{29}$$

where $\xi_o=(\alpha^2+c)^{1/2}$ (see the fourth of Eqns.(1) for $\eta=0$ and $y=c$), and r ranges in the interval $\alpha^2\le r\le(2h-c)$. Using these formulae, the distributions of the normal stress components along the y-axis are plotted in Fig.7. As previously, in order to draw these diagrams, a strip of dimensions 2bx2h=(30x20) cm was considered and the x-axis was constantly located at a distance c=5 cm from the upper edge of the strip. Four different parabolic notch geometries were considered, with α= 0.25, 0.5, 1.0, 1.4 $cm^{1/2}$. The strip was stretched by a uniform distribution of tensile stress σ_o=10 MPa on its lateral edges. The stress variations were plotted again in an appropriate scale to adjust to the strip dimensions for a better overview (obviously, the results in Fig.7 concerning the strips with for α=0.25, 0.5 and 1.0 $cm^{1/2}$, coincide with those in Figs.4 and 5, as they are essentially based on the same full-field formulae, given in the Appendix, reduced now to Eqns.(27, 28)).

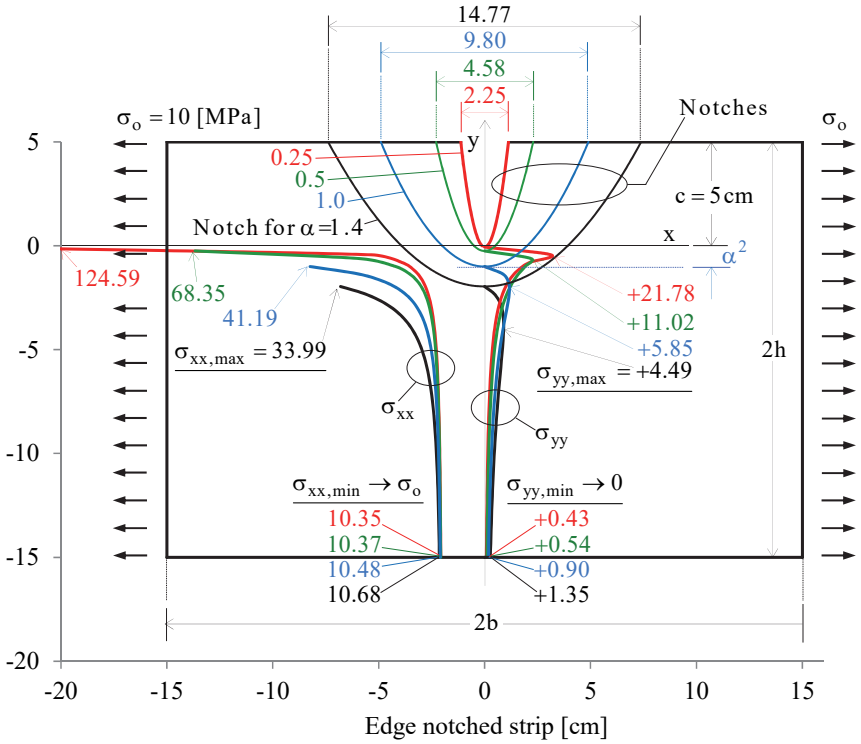

Figure 7: The variation of σ_{xx} and σ_{yy} stress components along the notch bisector (y-axis), for four notch dimensions.

The stress field at the base (tip) of the notch and the stress concentration k

In the edge-notched strip, uniaxially stretched normally to the axis of symmetry of the notch (i.e., for the "mode I" notch), the main interest is focused on the point at the base (tip) of the notch, where a significant stress concentration is expected

to appear, governing, thus, the failure of the strip. In this context, setting $r=\alpha^2$ in Eqn.(28) yields $\sigma_{yy}=0$, while Eqn.(27) provides the critical tensile stress $\sigma_{xx,cr}$ at the tip $(0, -\alpha^2)$ of the notch, as:

$$\sigma_{xx,cr} = \sigma_o \left(1 + \frac{4\xi_o}{\pi\alpha} \right) \tag{30}$$

Taking into account that by the third of Eqns.(1), $\xi_o = x_o / 2\alpha$, and that by Eqn.(2) $x_o = 2\alpha\sqrt{\alpha^2 + c}$, one obtains:

$$\sigma_{xx,cr} = \sigma_o \left(1 + \frac{4}{\pi\alpha}\sqrt{c + \alpha^2} \right) \tag{31}$$

In turn, the stress concentration factor, k, at the tip of the blunt (parabolic) notch is given by the simple expression:

$$k = \frac{\sigma_{xx,cr}}{\sigma_o} = 1 + \frac{4}{\pi\alpha}\sqrt{c + \alpha^2} \tag{32}$$

From Eqn.(32) the obvious conclusion is drawn that k is proportional to the 1/2 power of the depth $(c+\alpha^2)$ of the notch. The strongest dependence of k is on α, which, apart from the depth, dictates the sharpness of the notch base. The smaller the value of α, the higher the sharpness of the notch tip, reaching for $\alpha \to 0$ the limiting case of the 'mathematical' edge crack. In the latter case, the Stress Concentration concept shall give its place to the Stress Intensity one and the related Mode-I stress intensity factor K_I concept at the crack tip, which clearly constitutes a special limiting case of the present solution. For a fixed value c=5 cm, the dependence of k on α, which rules the depth (length) $(c+\alpha^2)$ and span $2x_o$ of the notch, is shown in Fig.8. Clearly, k increases rapidly after a value α of about 0.60.
The parameter c is also of crucial importance for the numerical values of k, however, it should be dealt with caution since values of c higher than that considered here, could lead to undesirable bending effects which must be taken into account in the analytical solution. In any case, such effects can be pretty well confronted by assuming long strips, in which case the present solution may be, also, applied without further modifications.

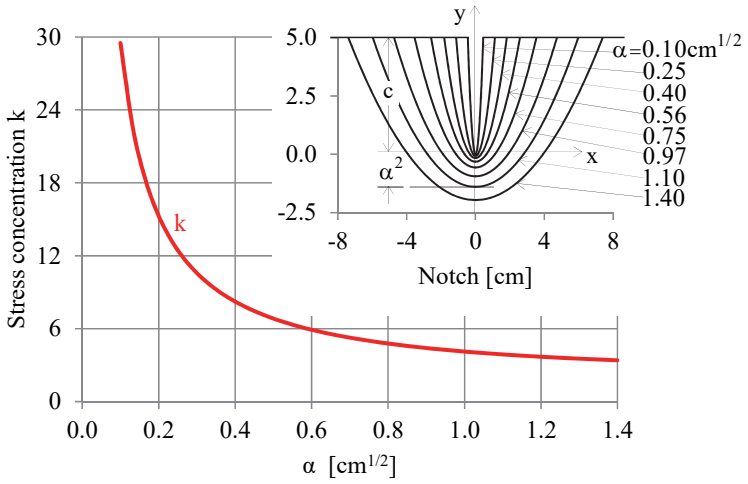

Figure 8: The stress concentration factor k versus the parameter α (dictating the dimensions of the notch).

DISCUSSION AND CONCLUSIONS

An alternative full-field and closed form, analytical solution was presented, for the plane problem of a finite strip that is weakened by a single edge notch of parabolic shape. The strip is assumed to be under uniform, uniaxial stretching. The analysis is based on an extension of the pioneering technique introduced by Mushkelishvili [13] for the solution of the problem of a perforated infinite strip, by considering firstly an intact strip and then 'neutralizing' (rendering it stress

free) a locus identical to that of the empty space of the perforation (by demanding the stresses to be zero along the perforation), transforming, thus, the intact infinite strip into a perforated one. Following this approach, an intact finite strip was firstly considered here under uniaxial tension. Then a part of the strip's area, resembling an edge parabolically-shaped notch, was 'neutralized' by superposing on its boundary an auxiliary stress field, opposite to the one developed due to the action of the tensile stress along the edges of the intact strip.

The specific procedure permitted determination of flexible (and relatively compact) formulae for the components of the stress field all over the strip. The main advantage of these formulae (apart from the fact that they are of closed form and full-field) is that they are relieved from the assumption of an 'infinite' medium. In other words, there is no need to assume that the dimensions of the notch are 'small' compared to those of the strip itself. The specific characteristic of the present solution permits relatively easy parametric analyses of various geometric configurations of the notch and the finite strip. It is mentioned, characteristically that by adjusting properly the parameters governing the shape of the parabolic notch, these formulae degenerate to the respective ones for a strip with a 'mathematical' crack.

The stress concentration factor, k, was proven to depend mainly on the parameter α, of the equation $x=2\alpha(\alpha^2+y)^{1/2}$ (the equation of the parabolic notch), namely the parameter that governs the sharpness of the notch. It was concluded that for values of α higher than 0.6 the stress concentration factor is relatively small, ranging (almost linearly) in a narrow interval $4<k<6$. From this limit on, the stress concentration factor starts increasing dramatically. It is mentioned characteristically that for $\alpha=0.2$ the respective value of the stress concentration factor is equal to about $k=15$.

The solution introduced is limited by the general assumption of linear elasticity, which, however, is a common assumption for the vast majority of studies dealing with notched strips. In this context it should be applied with consciousness in case ductile strips are considered, especially at load levels approaching the ones that will cause extensive yielding in the vicinity of the base (tip) of the notch. Moreover, it must be highlighted that the flanks of the notch are not linear segments (as it is commonly considered for U-shaped notches or for V-shaped notches with rounded tip).

In spite of these limitations, plotting the distribution of the stresses along some strategic loci, it was clearly indicated that the formulae obtained fulfill the boundary conditions imposed, even for notches of dimensions well comparable to those of the strip. The validity of the procedure introduced is further supported by the fact that the stress variations predicted are qualitative similar to the respective ones provided by well-established solutions [19], broadly used worldwide (although a direct quantitative comparison is not possible taking into account that the geometry of the notches considered there are not parabolically shaped but rather their flanks are linear). In this context, a project is already launched for the description of the stress filed in a parabolically notched strip using numerical approaches (by means of the Finite Element Method). Preliminary results, already available, are quite encouraging, indicating very satisfactory agreement with the ones obtained analytically [35]. Thus, taking into account the fact that the analytical procedure is relatively simple, and, in addition, the compactness of the equations describing the stress field (and especially the Stress Concentration Factor at the base (tip) of the notch), it can be stated that the alternative procedure introduced here may become a useful and flexible tool in hands of engineers working in the field of constructions.

REFERENCES

[1] Markides, C., Kourkoulis, S.K. (2023). Revisiting classical concepts of Linear Elastic Fracture Mechanics-Part I: The closing 'mathematical' crack in an infinite plate and the respective Stress Intensity Factors, Frat. Ed Integrità Strutt., 17(66), pp. 233–260. DOI: 10.3221/IGF-ESIS.66.15

[2] Inglis, C.E. (1913). Stresses in a plate due to the presence of cracks and sharp corners, Proc. Inst. Naval. Arch., 55, pp. 219–230.

[3] Cotterell, B. (2002). The past, present, and future of fracture mechanics, Eng. Fract. Mech., 69, pp. 533–553. DOI: 10. 1016/S0013-7944(01)00101-1.

[4] Griffith, A.A. (1920). The phenomenon of rupture and flow in solids. Phil. Trans. Roy. Soc. London, A221, pp. 163–198. DOI: 10.1098/rsta.1921.0006.

[5] Griffith, A.A. (1924). The theory of rupture. In: Biezeno, C.B., Burgers, J.M., editors. Proc. First Int. Congr. Appl. Mech. Delft: Technische Boekhandel en Drukkerij, pp. 55-63.

[6] Irwin, G.R. (1957). Analysis of stresses and strains near the end of a crack traversing a plate, J. Appl. Mech., 24, pp. 361–364. DOI: 10.1115/1.4011547.

[7] Westergaard, H.M. (1939). Bearing pressures and cracks: Bearing pressures through a slightly waved surface or through a nearly flat part of a cylinder, and related problems of cracks, J. Appl. Mech., 6, pp. A49-A53.

DOI: 10.1115/ 1.4008919.
[8] Williams, M.L. (1952). Stress singularities resulting from various boundary conditions in angular corners of plates in extension, J. Appl. Mech., 19(4), pp. 526–528. DOI: 10.1115/1.4010553.
[9] Williams, M.L. (1957). On the stress distribution at the base of a stationary crack, J. Appl. Mech., 24(1), pp. 109–114. DOI: 10.1115/1.4011454.
[10] Neuber, H. (1958). Theory of Notch Stresses, Springer-Verlag, Berlin.
[11] Carpenter, W.C. (1984). A collocation procedure for determining fracture mechanics parameters at a corner, Int. J. Fract., 24, pp. 255–266. DOI: 10.1007/BF00020740.
[12] Kolosov, G. (1935). An application of Complex Variables in the Theory of Elasticity, Moscow, Leningrad.
[13] Muskhelishvili, N.I. (1953). Some Basic Problems of the Mathematical Theory of Elasticity, Groningen, Noordhoff.
[14] Creager, M., Paris, P.C. (1967). Elastic field equations for blunt cracks with reference to stress corrosion cracking. Int.. J. Fract. Mech., 3, pp. 247–252. DOI: 10.1007/BF00182890.
[15] Glinka, G. Newport, A. (1987). Universal features of elastic notch-tip stress fields. Int. J. Fatigue, 9, pp. 143–150. DOI: 10.1016/0142-1123(87)90069-7.
[16] Lazzarin, P., Tovo, R. (1996). A unified approach to the evaluation of linear elastic stress fields in the neighborhood of cracks and notches. Int. J. Fract., 78, pp. 3–19. DOI: 10.1007/BF00018497.
[17] Nui, L.S., Chehimi, C., Pluvinage, G. (1994). Stress field near a large blunted tip V-notch and application of the concept of the critical notch stress intensity factor (NSIF) to the fracture toughness of very brittle materials, Eng. Fract. Mech., 49(3), pp. 325–335. DOI: 10.1016/0013-7944(94)90262-3.
[18] Atzori, B., Lazzarin, P., Marchioro, M. (1988). Fatigue resistance of welded lap joints with sheets of different thickness, Riv. Ital. Saldatura, 40(3), pp. 227–232.
[19] Filippi, S., Lazzarin, P., Tovo, R. (2002). Developments of some explicit formulas useful to describe elastic stress fields ahead of notches in plates, Int. J. Solids Struct., 39, pp. 4543–4565. DOI: 10.1016/S0020-7683(02)00342-6.
[20] Atzori, B., Lazzarin, P, Filippi S. (2001). Cracks and notches: analogies and differences of the relevant stress distributions and practical consequences in fatigue limit predictions, Int. J. Fatigue, 23(4), pp. 355–362. DOI: 10.1016/ S0142-1123(00)00107-9.
[21] Filippi, S., Lazzarin, P. (2004). Distributions of the elastic principal stress due to notches in finite size plates and rounded bars uniaxially loaded, Int. J. Fatigue 26, pp. 377–391. DOI: 10.1016/j.ijfatigue.2003.06.001.
[22] Lazzarin, P., Filippi S. (2006). A generalized stress intensity factor to be applied to rounded V-shaped notches, Int. J. Solids Struct., 43, pp. 2461–2478. DOI: 10.1016/j.ijsolstr.2005.03.007.
[23] Gómez, F.J., Elices, M., Berto, F., Lazzarin, P. (2008). A generalized notch stress intensity factor for U-notched components loaded under mixed mode, Eng. Fract. Mech., 75(16), pp. 4819–4833. DOI: 10.1016/j.engfracmech.2008. 07.001
[24] Gómez, F.J., Elices, M., Berto, F., Lazzarin, P. (2009). Fracture of U-notched specimens under mixed mode: experimental results and numerical predictions, Eng. Fract. Mech., 76(2), pp. 236–249. DOI: 10.1016/j.engfracmech.2008.10.001
[25] Berto, F., Lazzarin, P. (2009). A review of the volume-based strain energy density approach applied to V-notches and welded structures, Theor. Appl. Fract. Mech., 52(3), pp. 183–194. DOI: 10.1016/j.tafmec.2009.10.001
[26] Berto, F., Lazzarin, P., Marangon, C. (2012). Brittle fracture of U-notched graphite plates under mixed mode loading. Mater. Des., 41, pp. 421–432. DOI: 10.1016/j.matdes.2012.05.022.
[27] Lazzarin, P., Campagnolo, A., Berto, F. (2014). A comparison among some recent energy-and stress-based criteria for the fracture assessment of sharp V-notched components under Mode I loading, Theor. Appl. Fract. Mech., 71, pp. 21–30. DOI: 10.1016/j.tafmec.2014.03.001.
[28] Torabi, A.R., Berto, F., Razavi, S.M.J. (2018). Tensile failure prediction of U-notched plates under moderate-scale and large-scale yielding regimes, Theor. Appl. Fract. Mech., 97, pp. 434-439. DOI: 10.1016/j.tafmec.2017.07.009.
[29] Chen, D.H., Fan, X.L. (2019). Evaluation of the brittle failure of blunt U-shaped notch under mode I loading, Eng. Fract. Mech., 214, pp. 40–61. DOI: 10.1016/j.engfracmech.2019.04.022.
[30] Ghadirian, H.R., Akbardoost, J., Zhaleh, A. R. (2019). Fracture analysis of rock specimens weakened by rounded-V and U-shaped notches under pure mode I loading, Int. J. Rock Mech. Min. Sci., 123, 104103. DOI: doi.org/10.1016/ j.ijrmms.2019.104103
[31] Sangsefidi, M., Akbardoost, J., Mesbah, M. (2020). Experimental and theoretical fracture assessment of rock-type U-notched specimens under mixed mode I/II loading, Eng. Fract. Mech., 230, 106990. DOI: 10.1016/j.engfracmech. 2020.106990.

[32] Torabi, A. R., Shahbaz, S., Ayatollahi, M.R. (2023). Fracture assessment of U-notched diagonally loaded square plates additively manufactured from ABS with different raster orientations. Eng. Struct., 292, 116537. DOI: 10.1016/j.engstruct.2023.116537.

[33] Bagheri, P., Torabi, A.R., Bahrami, B. (2023). A new strategy for predicting fracture of U-notched specimens made of Al-6061-T6 and Al-5083 using extended finite element method, Fatigue Fract. Eng. Mater. Struct., 46(9), pp. 3404–3416. DOI: 10.1111/ffe.14086.

[34] Alshaya, A.A. (2023). A developed hybrid experimental–analytical method for thermal stress analysis of a deep U-notched plate. Theor. Appl. Fract. Mech., 124, 103753. DOI: 10.1016/j.tafmec.2023.103753.

[35] Kourkoulis, S.K., Markides Ch.F, Pasiou, E.D (2024). A combined analytical and numerical approach to the problem of the stress- and displacement-fields in finite strips weakened by parabolically shaped notches (under review).

APPENDIX

The formulae for the components of the stress field at any point (r, θ) of a strip of finite dimensions, weakened by a parabolically-shaped stress-free edge notch, assuming that it is subjected to uniform uniaxial tension σ_o, applied normally to the axis of symmetry of the notch:

$$
\begin{aligned}
\sigma_{xx} = \sigma_o + \frac{\sigma_o}{\pi}\Bigg\{ & \frac{\alpha}{\sqrt{r}}\left[\frac{1}{4\sqrt{2}}\left(\cos\frac{\theta}{2}+\sin\frac{\theta}{2}+\cos\frac{5\theta}{2}+\sin\frac{5\theta}{2}\right)+\frac{\alpha^2}{r\sqrt{2}}\left(\cos\frac{3\theta}{2}-\sin\frac{3\theta}{2}\right)\right]\cdot \\
& \cdot\log\sqrt{\frac{\left[\sqrt{\frac{r}{2}}\left(\cos\frac{\theta}{2}+\sin\frac{\theta}{2}\right)-\xi_o\right]^2+\left[\sqrt{\frac{r}{2}}\left(\sin\frac{\theta}{2}-\cos\frac{\theta}{2}\right)+\alpha\right]^2}{\left[\sqrt{\frac{r}{2}}\left(\cos\frac{\theta}{2}+\sin\frac{\theta}{2}\right)+\xi_o\right]^2+\left[\sqrt{\frac{r}{2}}\left(\sin\frac{\theta}{2}-\cos\frac{\theta}{2}\right)+\alpha\right]^2}} \qquad \left(\begin{array}{c}\xi_o=\sqrt{\alpha^2+c}\\ r=\sqrt{x^2+y^2},\quad \theta=\tan^{-1}\frac{y}{x}\end{array}\right) \\
& +\frac{\alpha}{\sqrt{r}}\left[\frac{\sqrt{r}}{\alpha}+\frac{1}{4\sqrt{2}}\left(\sin\frac{\theta}{2}-\cos\frac{\theta}{2}+\sin\frac{5\theta}{2}-\cos\frac{5\theta}{2}\right)+\frac{\alpha^2}{r\sqrt{2}}\left(\cos\frac{3\theta}{2}+\sin\frac{3\theta}{2}\right)\right]\cdot \\
& \cdot\left[\tan^{-1}\frac{\sqrt{\frac{r}{2}}\left(\sin\frac{\theta}{2}-\cos\frac{\theta}{2}\right)+\alpha}{\sqrt{\frac{r}{2}}\left(\cos\frac{\theta}{2}+\sin\frac{\theta}{2}\right)-\xi_o}-\tan^{-1}\frac{\sqrt{\frac{r}{2}}\left(\sin\frac{\theta}{2}-\cos\frac{\theta}{2}\right)+\alpha}{\sqrt{\frac{r}{2}}\left(\cos\frac{\theta}{2}+\sin\frac{\theta}{2}\right)+\xi_o}+\left\{\begin{array}{c}-\pi\\ 0\end{array}\right\}\right] \\
& +\frac{\xi_o\sqrt{2}}{\sqrt{r}}\left[\frac{5}{4}\left(\cos\frac{\theta}{2}-\sin\frac{\theta}{2}\right)+\frac{\alpha^2}{r}\left(\cos\frac{3\theta}{2}+\sin\frac{3\theta}{2}\right)-\frac{1}{4}\left(\sin\frac{5\theta}{2}-\cos\frac{5\theta}{2}\right)\right] \\
& -\left[\frac{5\alpha}{4}-\frac{\alpha^3}{r}\sin\theta-\frac{1}{4}\sqrt{\frac{r}{2}}\sin 2\theta\left(\cos\frac{\theta}{2}+\sin\frac{\theta}{2}\right)+\frac{\alpha\cos 2\theta}{4}-\frac{1}{2}\left(\sqrt{\frac{r}{2}}\cos^2\theta+2\sqrt{2}\frac{\alpha^2}{\sqrt{r}}\right)\left(\cos\frac{\theta}{2}-\sin\frac{\theta}{2}\right)\right]\cdot \\
& \cdot\left[\frac{\sqrt{\frac{r}{2}}\left(\cos\frac{\theta}{2}+\sin\frac{\theta}{2}\right)-\xi_o}{\left[\sqrt{\frac{r}{2}}\left(\cos\frac{\theta}{2}+\sin\frac{\theta}{2}\right)-\xi_o\right]^2+\left[\sqrt{\frac{r}{2}}\left(\sin\frac{\theta}{2}-\cos\frac{\theta}{2}\right)+\alpha\right]^2}-\frac{\sqrt{\frac{r}{2}}\left(\cos\frac{\theta}{2}+\sin\frac{\theta}{2}\right)+\xi_o}{\left[\sqrt{\frac{r}{2}}\left(\cos\frac{\theta}{2}+\sin\frac{\theta}{2}\right)+\xi_o\right]^2+\left[\sqrt{\frac{r}{2}}\left(\sin\frac{\theta}{2}-\cos\frac{\theta}{2}\right)+\alpha\right]^2}\right] \\
& -\left[-\frac{\alpha^3}{r}\cos\theta-\frac{1}{4}\sqrt{\frac{r}{2}}\sin 2\theta\left(\sin\frac{\theta}{2}-\cos\frac{\theta}{2}\right)-\frac{\alpha\sin 2\theta}{4}-\frac{1}{2}\left(\sqrt{\frac{r}{2}}\cos^2\theta-2\sqrt{2}\frac{\alpha^2}{\sqrt{r}}\right)\left(\cos\frac{\theta}{2}+\sin\frac{\theta}{2}\right)\right]\cdot \\
& \cdot\left[\frac{\sqrt{\frac{r}{2}}\left(\sin\frac{\theta}{2}-\cos\frac{\theta}{2}\right)+\alpha}{\left[\sqrt{\frac{r}{2}}\left(\cos\frac{\theta}{2}+\sin\frac{\theta}{2}\right)-\xi_o\right]^2+\left[\sqrt{\frac{r}{2}}\left(\sin\frac{\theta}{2}-\cos\frac{\theta}{2}\right)+\alpha\right]^2}-\frac{\sqrt{\frac{r}{2}}\left(\sin\frac{\theta}{2}-\cos\frac{\theta}{2}\right)+\alpha}{\left[\sqrt{\frac{r}{2}}\left(\cos\frac{\theta}{2}+\sin\frac{\theta}{2}\right)+\xi_o\right]^2+\left[\sqrt{\frac{r}{2}}\left(\sin\frac{\theta}{2}-\cos\frac{\theta}{2}\right)+\alpha\right]^2}\right]\Bigg\}
\end{aligned}
\tag{A.1}
$$

$$\sigma_{yy}=\frac{\sigma_o}{\pi}\left\{\frac{\alpha}{\sqrt{r}}\left[\frac{7}{4\sqrt{2}}\left(\cos\frac{\theta}{2}+\sin\frac{\theta}{2}\right)-\frac{\alpha^2}{r\sqrt{2}}\left(\cos\frac{3\theta}{2}-\sin\frac{3\theta}{2}\right)-\frac{1}{4\sqrt{2}}\left(\cos\frac{5\theta}{2}+\sin\frac{5\theta}{2}\right)\right]\cdot\right.$$

$$\cdot\log\sqrt{\frac{\left[\sqrt{\frac{r}{2}}\left(\cos\frac{\theta}{2}+\sin\frac{\theta}{2}\right)-\xi_o\right]^2+\left[\sqrt{\frac{r}{2}}\left(\sin\frac{\theta}{2}-\cos\frac{\theta}{2}\right)+\alpha\right]^2}{\left[\sqrt{\frac{r}{2}}\left(\cos\frac{\theta}{2}+\sin\frac{\theta}{2}\right)+\xi_o\right]^2+\left[\sqrt{\frac{r}{2}}\left(\sin\frac{\theta}{2}-\cos\frac{\theta}{2}\right)+\alpha\right]^2}}\qquad\left(\begin{array}{c}\xi_o=\sqrt{\alpha^2+c}\\ r=\sqrt{x^2+y^2},\quad\theta=\tan^{-1}\frac{y}{x}\end{array}\right)$$

$$+\frac{\alpha}{\sqrt{r}}\left[\frac{\sqrt{r}}{\alpha}+\frac{7}{4\sqrt{2}}\left(\sin\frac{\theta}{2}-\cos\frac{\theta}{2}\right)-\frac{\alpha^2}{r\sqrt{2}}\left(\cos\frac{3\theta}{2}+\sin\frac{3\theta}{2}\right)-\frac{1}{4\sqrt{2}}\left(\sin\frac{5\theta}{2}-\cos\frac{5\theta}{2}\right)\right]\cdot$$

$$\cdot\left[\tan^{-1}\frac{\sqrt{\frac{r}{2}}\left(\sin\frac{\theta}{2}-\cos\frac{\theta}{2}\right)+\alpha}{\sqrt{\frac{r}{2}}\left(\cos\frac{\theta}{2}+\sin\frac{\theta}{2}\right)-\xi_o}-\tan^{-1}\frac{\sqrt{\frac{r}{2}}\left(\sin\frac{\theta}{2}-\cos\frac{\theta}{2}\right)+\alpha}{\sqrt{\frac{r}{2}}\left(\cos\frac{\theta}{2}+\sin\frac{\theta}{2}\right)+\xi_o}+\left\{\begin{array}{c}-\pi\\0\end{array}\right\}\right]\qquad(A.2)$$

$$+\frac{\xi_o\sqrt{2}}{\sqrt{r}}\left[\frac{3}{4}\left(\cos\frac{\theta}{2}-\sin\frac{\theta}{2}\right)+\frac{\alpha^2}{r}\left(\cos\frac{3\theta}{2}+\sin\frac{3\theta}{2}\right)+\frac{1}{4}\left(\sin\frac{5\theta}{2}-\cos\frac{5\theta}{2}\right)\right]$$

$$+\left[\frac{5\alpha}{4}-\frac{\alpha^3}{r}\sin\theta+\frac{\alpha\cos2\theta}{4}-\frac{1}{4}\sqrt{\frac{r}{2}}\sin2\theta\left(\cos\frac{\theta}{2}+\sin\frac{\theta}{2}\right)-\frac{1}{2}\left(\sqrt{\frac{r}{2}}\cos^2\theta+2\sqrt{2}\frac{\alpha^2}{\sqrt{r}}\right)\left(\cos\frac{\theta}{2}-\sin\frac{\theta}{2}\right)\right]\cdot$$

$$\cdot\left[\frac{\sqrt{\frac{r}{2}}\left(\cos\frac{\theta}{2}+\sin\frac{\theta}{2}\right)-\xi_o}{\left[\sqrt{\frac{r}{2}}\left(\cos\frac{\theta}{2}+\sin\frac{\theta}{2}\right)-\xi_o\right]^2+\left[\sqrt{\frac{r}{2}}\left(\sin\frac{\theta}{2}-\cos\frac{\theta}{2}\right)+\alpha\right]^2}-\frac{\sqrt{\frac{r}{2}}\left(\cos\frac{\theta}{2}+\sin\frac{\theta}{2}\right)+\xi_o}{\left[\sqrt{\frac{r}{2}}\left(\cos\frac{\theta}{2}+\sin\frac{\theta}{2}\right)+\xi_o\right]^2+\left[\sqrt{\frac{r}{2}}\left(\sin\frac{\theta}{2}-\cos\frac{\theta}{2}\right)+\alpha\right]^2}\right]$$

$$+\left[-\frac{\alpha^3}{r}\cos\theta-\frac{\alpha\sin2\theta}{4}-\frac{1}{4}\sqrt{\frac{r}{2}}\sin2\theta\left(\sin\frac{\theta}{2}-\cos\frac{\theta}{2}\right)-\frac{1}{2}\left(\sqrt{\frac{r}{2}}\cos^2\theta-2\sqrt{2}\frac{\alpha^2}{\sqrt{r}}\right)\left(\cos\frac{\theta}{2}+\sin\frac{\theta}{2}\right)\right]\cdot$$

$$\left.\cdot\left[\frac{\sqrt{\frac{r}{2}}\left(\sin\frac{\theta}{2}-\cos\frac{\theta}{2}\right)+\alpha}{\left[\sqrt{\frac{r}{2}}\left(\cos\frac{\theta}{2}+\sin\frac{\theta}{2}\right)-\xi_o\right]^2+\left[\sqrt{\frac{r}{2}}\left(\sin\frac{\theta}{2}-\cos\frac{\theta}{2}\right)+\alpha\right]^2}-\frac{\sqrt{\frac{r}{2}}\left(\sin\frac{\theta}{2}-\cos\frac{\theta}{2}\right)+\alpha}{\left[\sqrt{\frac{r}{2}}\left(\cos\frac{\theta}{2}+\sin\frac{\theta}{2}\right)+\xi_o\right]^2+\left[\sqrt{\frac{r}{2}}\left(\sin\frac{\theta}{2}-\cos\frac{\theta}{2}\right)+\alpha\right]^2}\right]\right\}$$

$$\sigma_{xy}=\frac{\sigma_o}{\pi}\left\{\frac{\alpha}{\sqrt{r}}\left[\frac{3}{4\sqrt{2}}\left(\cos\frac{\theta}{2}-\sin\frac{\theta}{2}\right)+\frac{\alpha^2}{r\sqrt{2}}\left(\cos\frac{3\theta}{2}+\sin\frac{3\theta}{2}\right)+\frac{1}{4\sqrt{2}}\left(\sin\frac{5\theta}{2}-\cos\frac{5\theta}{2}\right)\right]\cdot\right.$$

$$\cdot\log\sqrt{\frac{\left[\sqrt{\frac{r}{2}}\left(\cos\frac{\theta}{2}+\sin\frac{\theta}{2}\right)-\xi_o\right]^2+\left[\sqrt{\frac{r}{2}}\left(\sin\frac{\theta}{2}-\cos\frac{\theta}{2}\right)+\alpha\right]^2}{\left[\sqrt{\frac{r}{2}}\left(\cos\frac{\theta}{2}+\sin\frac{\theta}{2}\right)+\xi_o\right]^2+\left[\sqrt{\frac{r}{2}}\left(\sin\frac{\theta}{2}-\cos\frac{\theta}{2}\right)+\alpha\right]^2}}\qquad\left(\begin{array}{c}\xi_o=\sqrt{\alpha^2+c}\\ r=\sqrt{x^2+y^2},\quad\theta=\tan^{-1}\frac{y}{x}\end{array}\right)$$

$$+\frac{\alpha}{\sqrt{r}}\left[\frac{3}{4\sqrt{2}}\left(\sin\frac{\theta}{2}+\cos\frac{\theta}{2}\right)+\frac{\alpha^2}{r\sqrt{2}}\left(\sin\frac{3\theta}{2}-\cos\frac{3\theta}{2}\right)-\frac{1}{4\sqrt{2}}\left(\sin\frac{5\theta}{2}+\cos\frac{5\theta}{2}\right)\right]\cdot$$

$$\cdot\left[\tan^{-1}\frac{\sqrt{\frac{r}{2}}\left(\sin\frac{\theta}{2}-\cos\frac{\theta}{2}\right)+\alpha}{\sqrt{\frac{r}{2}}\left(\cos\frac{\theta}{2}+\sin\frac{\theta}{2}\right)-\xi_o}-\tan^{-1}\frac{\sqrt{\frac{r}{2}}\left(\sin\frac{\theta}{2}-\cos\frac{\theta}{2}\right)+\alpha}{\sqrt{\frac{r}{2}}\left(\cos\frac{\theta}{2}+\sin\frac{\theta}{2}\right)+\xi_o}+\begin{Bmatrix}-\pi\\0\end{Bmatrix}\right]$$

$$+\frac{\xi_o\sqrt{2}}{\sqrt{r}}\left[\frac{\cos\theta}{2}\left(\cos\frac{3\theta}{2}+\sin\frac{3\theta}{2}\right)+\frac{\alpha^2}{r}\left(\cos\frac{3\theta}{2}-\sin\frac{3\theta}{2}\right)\right]$$

$$-\left[\frac{\alpha^3}{r}\cos\theta+\frac{\alpha\sin 2\theta}{4}+\frac{1}{4}\sqrt{\frac{r}{2}}\left(\cos\frac{\theta}{2}+\sin\frac{\theta}{2}+\cos\frac{3\theta}{2}-\sin\frac{3\theta}{2}\right)-\frac{\alpha^2\sqrt{2}}{\sqrt{r}}\left(\cos\frac{\theta}{2}+\sin\frac{\theta}{2}\right)\right]\cdot \tag{A.3}$$

$$\cdot\left[\frac{\sqrt{\frac{r}{2}}\left(\cos\frac{\theta}{2}+\sin\frac{\theta}{2}\right)-\xi_o}{\left[\sqrt{\frac{r}{2}}\left(\cos\frac{\theta}{2}+\sin\frac{\theta}{2}\right)-\xi_o\right]^2+\left[\sqrt{\frac{r}{2}}\left(\sin\frac{\theta}{2}-\cos\frac{\theta}{2}\right)+\alpha\right]^2}-\frac{\sqrt{\frac{r}{2}}\left(\cos\frac{\theta}{2}+\sin\frac{\theta}{2}\right)+\xi_o}{\left[\sqrt{\frac{r}{2}}\left(\cos\frac{\theta}{2}+\sin\frac{\theta}{2}\right)+\xi_o\right]^2+\left[\sqrt{\frac{r}{2}}\left(\sin\frac{\theta}{2}-\cos\frac{\theta}{2}\right)+\alpha\right]^2}\right]$$

$$-\left[\frac{5\alpha}{4}-\frac{\alpha^3}{r}\sin\theta+\frac{\alpha\cos 2\theta}{4}-\frac{1}{4}\sqrt{\frac{r}{2}}\left(\cos\frac{\theta}{2}-\sin\frac{\theta}{2}+\cos\frac{3\theta}{2}+\sin\frac{3\theta}{2}\right)-\frac{\alpha^2\sqrt{2}}{\sqrt{r}}\left(\cos\frac{\theta}{2}-\sin\frac{\theta}{2}\right)\right]\cdot$$

$$\cdot\left[\frac{\sqrt{\frac{r}{2}}\left(\sin\frac{\theta}{2}-\cos\frac{\theta}{2}\right)+\alpha}{\left[\sqrt{\frac{r}{2}}\left(\cos\frac{\theta}{2}+\sin\frac{\theta}{2}\right)-\xi_o\right]^2+\left[\sqrt{\frac{r}{2}}\left(\sin\frac{\theta}{2}-\cos\frac{\theta}{2}\right)+\alpha\right]^2}-\frac{\sqrt{\frac{r}{2}}\left(\sin\frac{\theta}{2}-\cos\frac{\theta}{2}\right)+\alpha}{\left[\sqrt{\frac{r}{2}}\left(\cos\frac{\theta}{2}+\sin\frac{\theta}{2}\right)+\xi_o\right]^2+\left[\sqrt{\frac{r}{2}}\left(\sin\frac{\theta}{2}-\cos\frac{\theta}{2}\right)+\alpha\right]^2}\right]\Bigg\}$$